ORIGINAL RESEARCH

Measuring Water Distribution in the Heart: Preventing Edema Reduces Ischemia–Reperfusion Injury

Mireia Andrés-Villarreal, MD; Ignasi Barba, PhD; Marcos Poncelas, PhD; Javier Inserte, PhD; José Rodriguez-Palomares, MD, PhD; Victor Pineda, MD, PhD; David Garcia-Dorado, MD, PhD, FAHA

***Background*—**Edema is present in many heart diseases, and differentiation between intracellular (ICW) and extracellular (ECW) myocardial water compartments would be clinically relevant. In this work we developed a magnetic resonance imaging–based method to differentiate ICW and ECW and applied it to analyze ischemia–reperfusion–induced edema.

***Methods and Results*—**Isolated rat hearts were perfused with gadolinium chelates as a marker of extracellular space. Total water content was measured by desiccation. Gadolinium quantification provided ECW, and ICW was calculated by subtraction of ECW from total water content. In separate experiments, T1, T2, diffusion-weighted imaging and proton-density parameters were measured in isolated saline-perfused hearts. In in-situ rat hearts, ECW and ICW were 79±10 mL and 257±8 mL of water per 100 g of dry tissue, respectively. After perfusion for 40 minutes, ECW increased by 92.4±3% without modifying ICW (−1±3%). Hyposmotic buffer (248 mOsm/L) increased ICW by 16.7±2%, while hyperosmotic perfusion (409 mOsm/L) reduced ICW by 26.5±3%. Preclinical imaging showed good correlation between T2 and diffusion-weighted imaging with ECW, and proton-density correlated with total water content. Ischemia–reperfusion resulted in marked myocardial edema at the expense of ECW, because of cellular membrane rupture. When cell death was prevented by blebbistatin, water content and distribution were similar to normoxic perfused hearts. Furthermore, attenuation of intracellular edema with hyperosmotic buffer reduced cell death.

***Conclusions*—**We devised a method to determine edema and tissue water distribution. This method allowed us to demonstrate a role of edema in reperfusion-induced cell death and could serve as a basis for the study of myocardial water distribution using magnetic resonance imaging. **(*J Am Heart Assoc*. 2016;5:e003843 doi: 10.1161/JAHA.116.003843)**

Key Words: edema • gadolinium chelates • hyperosmotic reperfusion • ischemia • magnetic resonance imaging

Myocardial edema appears in many heart diseases and pathologic situations involving the heart: ischemic syndromes,[1–3] cardiac inflammation (myocarditis and graft rejection),[4,5] and mechanical overload secondary to valve disease or arterial hypertension.[6,7] Acute myocardial infarction and apical ballooning syndrome are characterized by significant myocardial edema in the ischemic[8–10] or transiently dyskinetic segments.[1,11,12] Literature suggests that intracellular myocardial edema may have a role in cardiomyocyte cell death,[13] myocardial stunning,[14,15] and in the nonreflow phenomenon.[16–19] On the other hand, laboratory experiments suggest that interstitial edema secondary to pressure overload may be related to the genesis of myocardial fibrosis,[20] and to be one of the underlying mechanisms of diastolic dysfunction.[21,22]

Magnetic resonance imaging (MRI) consists of measuring protons and their properties in a 3-dimensional space and turning the information into images. Heart MRI signal comes mainly from water protons; thus, it is the method of choice for the study of edema. T1 values have been used to measure extracellular volume,[23] but the method requires some assumptions, such as a dynamic steady state for gadolinium (Gd)-containing extracellular marker that may not be adequate in certain pathological circumstances.

Edematous areas in the heart appear bright in T2-weighted images because the T2 relaxation time becomes longer.[11] T2-weighted cardiac MRI is increasingly being used in clinical practice as a diagnostic tool and also to retrospectively evaluate the area at risk (myocardium that suffered ischemia during transient coronary occlusion) as a variable to normalize infarct size limitation as a primary end point in clinical trials of

From the Cardiology Department, Vall d'Hebron University Hospital and Research Institute, Universitat Autònoma de Barcelona, Spain (M.A.-V., I.B., M.P., J.I., J.R.-P., D.G.-D.); Institut Diagnostic per la Imatge, Barcelona, Spain (M.A.-V., V.P.).

Correspondence to: Ignasi Barba, PhD, or David Garcia-Dorado, MD, PhD, FAHA, Cardiology Department, Hospital Vall d'Hebron, Passeig de la Vall d'Hebron 119, Barcelona 08035, Spain. E-mails: ignasi.barba@vhir.org; dgdorado@vhebron.net

Received May 4, 2016; accepted October 5, 2016.

reperfusion injury.[24] However, using T2-weighted images is subject to limitations including acquisition timing dependence of the results[25] and influence of treatments as pre-, post-, or remote ischemic conditioning.

Information regarding myocardial water distribution may shed light into the pathophysiology of various processes including reperfusion injury. However, current experimental methods to determine water distribution between intra- and extracellular tissue compartments are based on radionuclide labeling of macromolecules with suitable diffusion properties[8–10] that are difficult to translate to clinical practice.

In this study we devised a reliable method to determine myocardial water distribution using MRI, which could serve as a basis for the development of methods with clinical application, and applied it to investigate whether edema does contribute to cardiomyocyte death after ischemia–reperfusion (IR).

Table 1. Composition and Osmolarity for the Different Buffers Used in This Work

	Krebs Henseleit	Hyposmotic Modified KH	Hyperosmotic Modified KH
Osmolarity, mOsm/L	308	248	409
NaCl	118	88	118
KCl	4.7	4.7	4.7
Mg_2SO_4	1.2	1.2	1.2
$NaHCO_3$	25	25	25
$CaCl_2$	1.8	1.8	1.8
KH_2PO_4	1.2	1.2	1.2
Glucose	11	11	11
Mannitol			101

Units in mmol/L. KH indicates Krebs-Henseleit.

Methods

Animals

All the experiments were carried out with male Sprague-Dawley rats weighting 300 to 350 g. Animals were cared for according to the European laws and to the instructions provided in the "Guide for the Care and Use of Laboratory Animals" published by the US National Institutes of Health (NIH Publication No. 85-23, revised 1996). The experimental protocols were approved by the Animal Ethics Committee at "Vall d'Hebron Institut de Recerca."

In Situ Rat Heart Experiments

In situ experiments were performed in 4 animals. Anesthesia was induced with 5% isoflurane and maintained with isoflurane 2%. ECG and rectal temperature were continuously monitored during the experiment as well as appropriate anesthetic level. The jugular vein and the carotid artery were cannulated and a solution of gadobutrol 1 mmol/mL was perfused for 5 minutes at 0.35 μL/min per gram through the jugular vein. This perfusion rate was established in order to achieve a Gd plasma concentration between 1 and 10 mmol/L, assuming a blood volume of around 50 to 70 mL/kg and cardiac output 121 mL/kg per minute and a volume of distribution in steady state of 0.20 L/kg. A blood sample from the carotid artery was obtained during the last 30 s of Gd-BT-DO3A perfusion, just before the excision of the heart. The removed heart was washed in NaCl 0.9% at 4°C.

Saline-Perfused Isolated Rat Heart Experiments

Animals were anesthetized with an intraperitoneal pentobarbital overdose injection (100 mg/kg). Once deep unconsciousness was achieved, hearts were removed by a subxiphoidal incision and thoracotomy. Hearts were washed in cold (4°C) saline solution (NaCl 0.9%) and hung at the cannula of a continuous perfusion system through the ascending aorta. Hearts were retrogradely perfused with continuously oxygenated buffer at 37°C. Flow was adjusted to obtain a perfusion pressure between 45 and 60 mm Hg. A balloon was allocated at the left ventricle chamber and inflated to achieve 8 to 12 mm Hg of telediastolic pressure. Left ventricle developed pressure and perfusion pressure were monitored throughout the experiment.[26]

In order to evaluate the effects of different buffer osmolarities in water distribution during normoperfusion, we used 3 perfusion buffers with varying osmolarity to induce different patterns of water distribution between the intracellular and extracellular compartments. Control hearts (n=8) were perfused with Krebs-Henseleit buffer at 308 mOsm/L. Hyposmotic experiments (n=9) were conducted in low-NaCl to obtain an osmolarity of 248 mOsm/L, and mannitol (n=11) was added to obtain high osmolarity of 409 mOsm/L. In all cases pH was adjusted to 7.4 (see Table 1 for complete buffer composition).

In all cases, perfusion lasted for 40 minutes and during the last 5 minutes, Gd chelate (gadobutrol) was added to a final concentration of 1 mmol/L (Figure 1A); it was previously checked that after 3.5 minutes the concentration of Gd in the effluent achieved steady-state (data not shown).

I–R Protocols in the Crystalloid Perfused Isolated Rat Heart

Figure 1B shows the protocols designed to study the effects of edema in IR injury. The protocol included 30 minutes of perfusion (equilibration period) followed by 40 minutes of

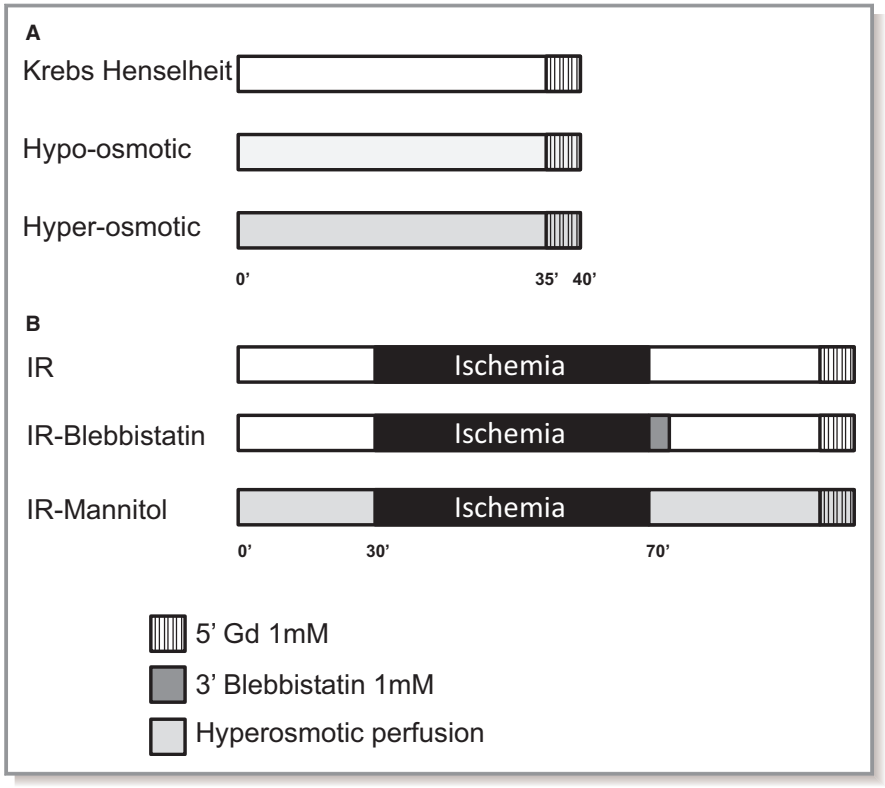

Figure 1. Perfusion protocols. A, Experiments with normoxic perfusion at different osmolarity: normosmotic Krebs-Henseleit (KH), hyposmotic low-NaCl modified KH and hyperosmotic mannitol modified KH. Gd was perfused during the last 5 minutes of perfusion. B, The perfusion protocols of the ischemia–reperfusion (IR) experiments: in all cases a 30-minute stabilization period preceded the 40 minutes of ischemia followed by 30 minutes of reperfusion. White bars correspond to Krebs Henseleit buffer; light gray, hyperosmotic buffer; dark gray to blebbistatin containing buffer and shadowed areas to gadolinium containing buffer. Samples for LDH quantification were taken during reperfusion. Blebbistatin was perfused during the first 3 minutes of reperfusion in the blebbistatin group. Hyperosmotic mannitol modified-KH buffer was perfused both during the stabilization period and reperfusion in the hyperosmotic IR group. In all cases 1 mmol/L Gd was added to the perfusion buffer during the last 5 minutes of reperfusion. LDH indicates lactate dehydrogenase.

ischemia at 37°C (perfusion discontinuation) and 30 minutes of reperfusion.

Three groups were analyzed: the control IR group with Krebs-Henseleit buffer (n=6), the blebbistatin-treated group (n=4), and the mannitol group (n=4). Blebbistatin prevents hypercontracture and cell death[27,28] and it has been used in this protocol to maintain intra- and extracellular space integrity by avoiding membrane rupture; blebbistatin was added during the first 3 minutes of reperfusion.[27]

Effluent samples were obtained during reperfusion to quantify infarct size by lactate-dehydrogenase (LDH) release. LDH is expressed as units 5 $min^{-1} \cdot g^{-1}$.

Measurement of Total Water Content

Once the hearts were removed from the perfusion system or, in the case of in situ experiments, washed in cold physiologic serum to remove excess blood, the surrounding excess water was carefully removed with the aid of a nylon membrane. Hearts were cut in 3 parts excluding the valve plane (apex and 2 symmetric sections of the basal portion, both containing similar amounts of right and left ventricle mass). Each portion was weighed and then freeze-dried overnight. After freeze-drying, samples were weighed again in order to obtain the dry mass. The difference between the fresh and the dry mass provided total water content (TWC) of each sample. Freeze-dried samples were stored at −20°C until Gd extraction.

Extracellular Water Content Measurement

Freeze-dried samples were micronized inside an assay tube using a spatula. Once micronized, 1 mL of miliQ water was added to the sample, vortex-shook, and let stand for 10 minutes at room temperature. Afterwards the sample

was centrifuged at 2000*g* for 5 minutes and the supernatant containing Gd was recovered. Only the first extraction was used for the final analysis, after checking that further extracts did not provide additional information about Gd content. Gd concentration in the effluent was measured at the time of heart removal in each experiment.

Gd measurement was based on the fact that Gd concentration proportionally shortens the spin-lattice relaxation time (T1).[29] To measure T1 in each sample, the extract was put into a 5-mm MR tube. Seven samples and 5 calibration line tubes (containing Gd at 0–0.5–0.6–0.8–1 mmol/mL) were allocated into the 40-mm MR coil for each measurement. Images were acquired in a vertical 9.4T magnet interfaced to a Bruker® (Madrid, Spain) Avance console. Sequence details: ET=4 ms, RT×9 (6.000–4.000–3.000–2.000–1.000–500–250–125–62.5) ms, where ET is echo time and RT repetition time matrix: 256×256-pixel resolution in a 30×30-mm window and slice thickness of 1.0 mm. For each sample, a region of interest at the center of the tube was obtained and the signal intensity was measured. This signal intensity was plotted against RT and fitted to an exponential function provided by Bruker software to obtain the T1 value. This function was used to calculate the concentration of Gd from measured T1 values.

In the case of the in situ experiments, Gd concentration in the animal serum was also analyzed. Arterial blood sample (0.3 mL) was obtained at the time of euthanizing and left to coagulate at room temperature. Afterwards the sample was centrifuged at 2000*g* for 10 minutes in order to obtain the serum, which was stored at −20°C until MR analysis.

MRI of Perfused and In Situ Hearts

In a separate set of experiments (n=4 for Krebs-Henseleit, hyposmotic, and hyperosmotic perfused groups), we measured T2, diffusion-weighted imaging, and proton-density values of rat hearts after saline perfusion without Gd. Nonperfused hearts (n=2) were removed from the animal and washed in cold physiologic serum before MRI measurements. T2 was measured with a spin-echo pulse sequence with a RT of 6000 ms and 16 echoes of 4 ms. Proton-density was defined as the voxel mean signal intensity of the first echo image obtained with a pulse-echo sequence with RT 10 000 ms and echo time of 4 ms and expressed as a percentage of the intensity of free water.

Diffusion-weighted images were acquired with a DtiEPI pulse sequence with ET set at 25 ms and RT at 3000 ms, and 7 b-values between 4 and 755 s/mm$^{2.}$

Infarct Size Measurement

In the isolated heart model, infarct size was estimated with the area under the curve of the LDH release during the reperfusion period as previously described.[30] LDH data are expressed as units of activity released per gram of dry weight during the first 5 minutes of reperfusion.

Statistical Analysis

Data were analyzed using ANOVA and Tukey's post hoc test by means of commonly available software (SPSS version 15 for Windows (SPSS Inc, Chicago, IL)). Correlation test was made by linear regression analysis using SigmaPlot software. Data were checked for normality using the Kolmogorov–Smirnov test. Differences with $P<0.05$ were considered statistically significant. Results are given as mean±SE.

Results

Heart hemodynamics during saline perfusion were similar between the different experimental protocols. IR induced extensive cell death (LDH: 353±67) in contrast to control perfusion (LDH: 56±16 $P<0.05$). Cell death was prevented by the use of blebbistatin during the first 3 minutes of reperfusion (LDH: 65±17, P=ns versus control).

$T1^{-1}$ and [Gd] showed a good linear correlation when [Gd] <5 mmol/L (r^2=0.997±0.0042; n=55 calibration curves), thus allowing adequate measurement of extracellular space. Correlation between LogT1 and [Gd] was linear for [Gd] <0.1 mmol/L.

Edema Distribution Studies

In situ hearts contained 336±5 mL water/100 g dry tissue, 257±8 mL/100 g of it were intracellular and the remaining 79±10 mL/100 g extracellular. Perfusion with Krebs-Henseleit buffer for 40 minutes induced edema (an increase of 19% of TWC) at the expense of extracellular myocardial water compartments (ECW) with preserved intracellular myocardial water compartments (ICW) content. In the normo-osmotic saline-perfused hearts, TWC was 406±6 mL/100 g ($P<0.001$), ECW 152±5 mL/100 g ($P<0.01$), and ICW 254±7 mL/100 g (P=ns versus in situ hearts).

Perfusion with hyposmotic buffer induced an additional 9% increase of TWC because of an 18% increase of the intracellular water compartment: TWC 444±2.6 mL/100 g ($P<0.01$), ECW 144±5.6 mL/100 g (P=ns), and ICW 300±5 mL/100 g ($P<0.01$). On the other hand, hyperosmotic perfusion decreased TWC by 10% at the expense solely of the ICW compartment (reduced by 26%): TWC 362±4.4 mL/100 g ($P<0.01$), ECW 172±6.5 mL/100 g (P=ns), and ICW 189±5.3 mL/100 g ($P<0.01$), suggesting water redistribution from the ICW space to the interstitium. All saline-perfused groups showed a significant increase of ECW as compared to in vivo hearts ($P<0.01$) but did not show significant differences

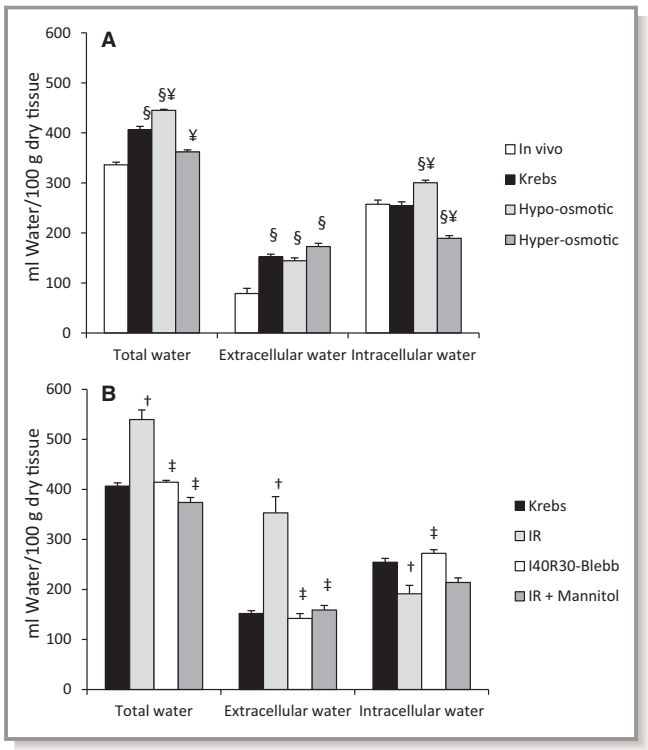

Figure 2. Myocardial water content and distribution. A, Water content (mL/100 g dry tissue) in the in situ (n=4) and normoxic perfused hearts (control Krebs-Henseleit [KH] n=8; hyposmotic n=9, hyperosmotic n=11). $^{§}P<0.05$ compared to nonperfused (in situ) heart. $^{¥}P<0.05$ compared to KH perfused hearts. B, Ischemia–reperfusion insulted hearts (IR group n=6, IR blebbistatin group n=4; IR mannitol group n=4) compared to KH normoxic perfused hearts. $^{†}P<0.05$ compared to KH perfused hearts. $^{‡}P<0.05$ compared to IR insulted hearts.

in ECW between them. Water content and distribution in the different groups is shown in Figure 2 and Table 2.

Hearts subjected to IR showed a marked increase in TWC in comparison to nonischemic saline-perfused hearts. The Gd-diffusible space (ECW) increased by 200 mL/100 g as compared to control perfused hearts; however, ICW was reduced after IR (Figure 2B). Total and extracellular water compartments showed a good linear correlation with the extent of cell death after IR injury measured as LDH release (r^2=0.9485, $P<0.01$, and r^2=0.8844, $P<0.01$, respectively) as shown in Figure 3.

Table 2. Water Content and Distribution During the Different Protocols

	TWC	ECWC	ICWC
In situ	336±5	79±10	257±8
KH 40′	406±6	152±5	243±13
Hyposmotic 40′	445±2	144±6	306±8
Hyperosmotic 40′	361±4	172±7	189±5
IR	539±19	353±32	191±17
IR-blebbistatin	414±4	142±10	272±7
IR-hyperosmotic	374±10	159±9	214±9

All data are in mL of water per 100 g of dry tissue. Values are expressed as mean±SD. ECWC indicates extracellular water content; ICWC, intracellular water content; IR, ischemia–reperfusion injury protocols; KH, Krebs-Henseleit; TWC, total water content.

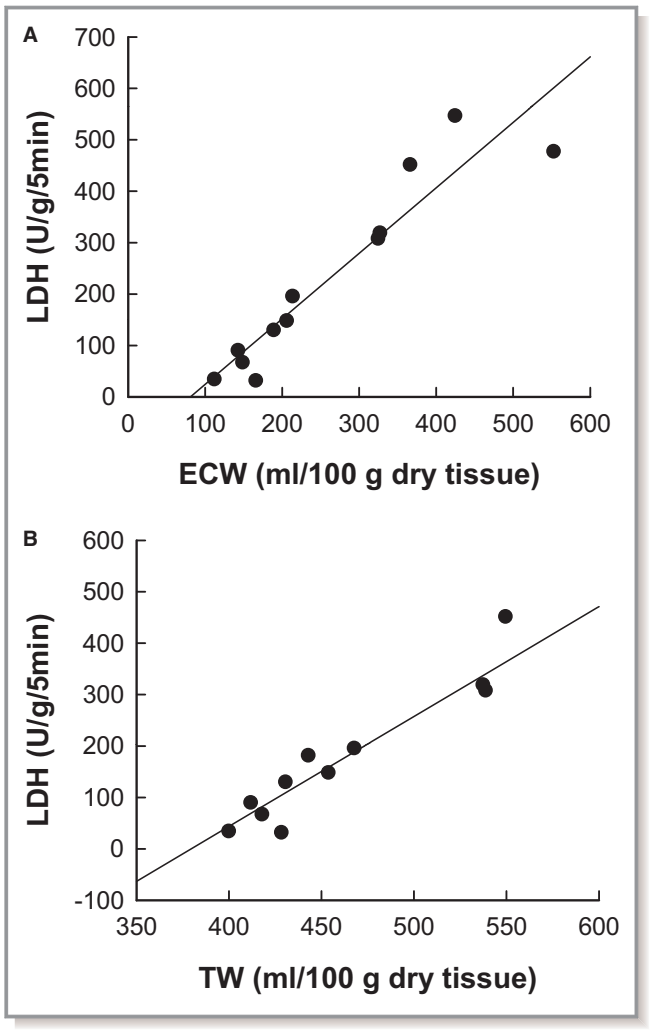

Figure 3. Graph showing the correlation between edema and cell death (n=12). A, Corresponds to the correlation between extracellular water and LDH while (B) shows total water content against cell death measured as LDH release. ECW indicates extracellular water; LDH, lactate dehydrogenase; TW, total water.

Preventing hypercontracture with blebbistatin markedly attenuated cell death induced by IR (LDH 353±67 versus 65±17, $P<0.05$) and edema (539±18 versus 414±4 mL/100 g, $P<0.05$) (Table 2). Likewise, reducing intracellular edema with the use of a hyperosmotic buffer prevented cell death (LDH 36±15; P=ns versus control).

MRI of Perfused and In Situ Hearts

In a separate set of experiments, we obtained MR images of the in situ and saline-perfused hearts under different osmotic

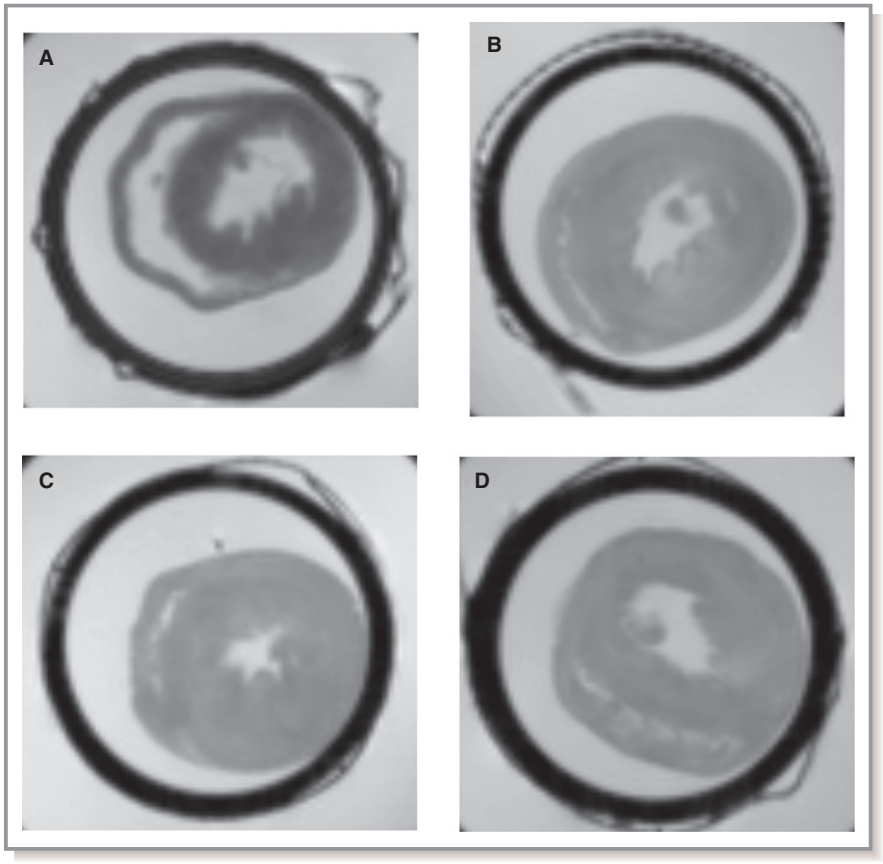

Figure 4. Ex-vivo images of rat hearts acquired with a RARE pulse sequence, TR 10 000 and TE 13 ms. A, Corresponds to a nonperfused heart, (B through D) to hearts perfused in the Langendorff system with hyperosmotic, normo-osmotic and hypo-osmotic buffers, respectively. Note that perfusion induces a high degree of edema. Hearts appear in black circles that correspond to plastic tubing used to center the organs. RARE indicates rapid acquisition with relaxation enhancement.

stress conditions (Figure 4), and found that T2 values showed good correlation with extracellular water content (r^2=0.993, P<0.01) while proton-density values correlated with total water content (r^2=0.988, P<0.01). On the other hand, T2 and proton-density showed poor correlation with total and extracellular water content, respectively (r^2=0.305 and 0.318, p=ns) (Figure 5). The diffusion-weighted imaging constant also showed a correlation with ECW although not as strong as T2 (r^2=0.893, P<0.01).

Discussion

In this work we presented a method based on extracellular space labeling using Gd that allows determination of water distribution in the myocardium. In this context, extracellular water is equivalent to the Gd diffusible space that includes intravascular and interstitial spaces. The method provided physiologically meaningful data on the effect of IR on intra- and extracellular water distribution. Comparison of the results obtained with this method with MRI variables indicates that T2 correlated with EWC while total water content correlated with proton-density. Data presented here support the notion that intracellular edema may contribute to cardiomyocyte death during initial reperfusion.

At present there is no "gold standard" to measure water content and distribution, but our measures based on Gd-chelates in intact heart are in close agreement with previous work done using radionuclide-labeled compounds.[31] The results presented here for in situ experiments are in close agreement with the literature data showing ECW values between 69 and 112 (mean value 95) mL/100 g dry tissue and ICW between 263 and 278 (mean value 271) mL/100 g dry tissue.[31] TWC in Langendorff-perfused rat hearts ranged from 429 to 784 mL/100 g dry tissue; ECW from 175 to 603 (mean value of 374) mL/100 g dry tissue, and ICW ranged from 181 to 253 (mean value of 224) mL/100 g dry tissue.[31] The highest variability was found in ECW content. One of the reasons leading to this great variability could be the removal of the buffer surrounding the heart; we found that this step is crucial in obtaining accurate and reproducible results.

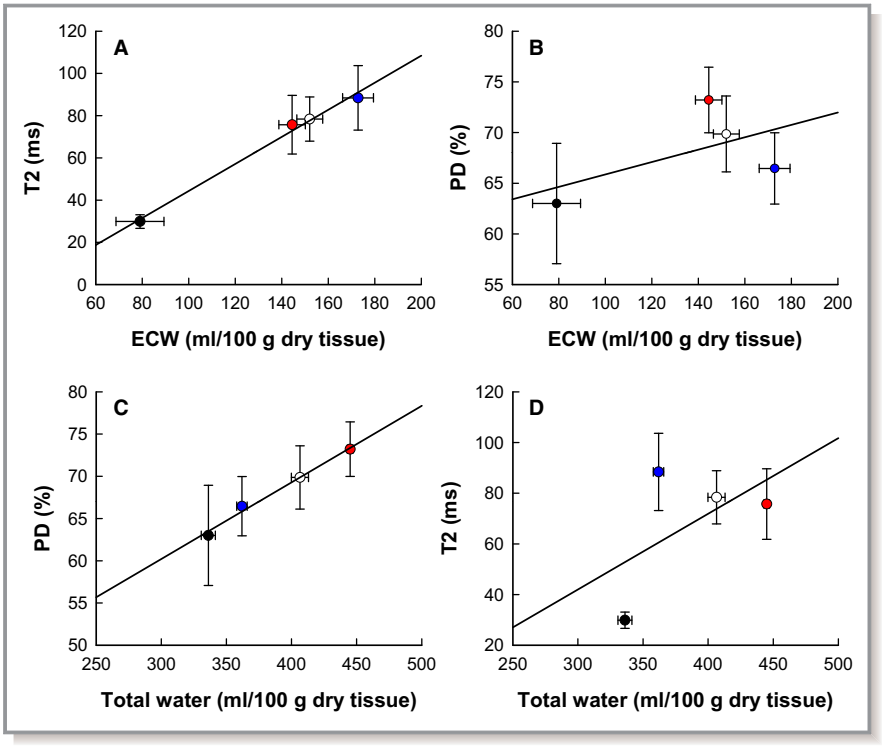

Figure 5. Correlation between MRI parameters and edema components (A) shows a good correlation between T2 and extracellular water while (B) shows that ECW does not correlate with proton-density. C, Corresponds to the correlation between proton-density and total water content and (D) is the correlation between proton-density and extracellular water. Black symbols correspond to in situ experiments, red to hypo-osmotic perfusion, white to normo-osmotic, and blue to hyper-osmotic perfusion protocols. Each point is the average of various experiments (n=4 each for MRI experiments, except for nonperfused group with n=2; n=4, 8, 9, 11 for in situ, control, hyposmotic, and hyperosmotic groups, respectively in the water content experiments; error bars show SE).

Early cell death during reperfusion occurs mainly through necrosis involving sarcolemmal rupture.[32] Our results show that intracellular space diminishes inversely proportional to IR injury, which is consistent with sarcolemmal rupture and intracellular space becoming accessible to Gd chelates. Prevention of cardiomyocyte death with myosin–actin inhibitors—both 2,3-butanedione monoxime[33,34] and the more specific blebbistatin[28]—also prevented intracellular space from becoming extracellular, proving that, at least part, the increase of extracellular edema is due to sarcolemmal rupture and Gd chelates having access to that space.

The contribution of reperfusion-induced cellular edema to cell death and myocardial infarct size was suggested over 2 decades ago[24] but has been a subject of controversy,[35] in part due to the lack of confirmation regarding the effects of hyperosmotic reperfusion on intra- and extracellular edema. In the present study we have been able to show that when ICW edema is selectively prevented with a hyperosmotic medium, sarcolemmal rupture and infarct size are reduced in isolated perfused hearts. The present findings clearly support a role for edema as a mechanism of cell death during IR injury.

Our ex-vivo imaging results showed a good correlation between T2 and, to a lesser extent, apparent diffusion-weighted imaging coefficient, with extracellular water. Proton-density correlated with total water content, pointing towards the possibility of measuring myocardial water distribution through MRI and to the application of this method in patients.

Previous reports have described a correlation between T2 and total water content in IR models.[32,36] After extensive myocardial infarction, cell membranes lose their integrity, and intra- and extracellular water compartments mix. In these circumstances T2 would also correlate with total water content. On the other hand, the present experimental approach does allow modifying water distribution and we are able to prevent cell membrane rupture; the increase in number of conditions studied allowed us to correlate T2 with extracellular water.

Conclusions

In conclusion, we describe a method to measure myocardial edema distribution using MRI based on the kinetics and

magnetic properties of Gd chelates. This technique may be very useful in preclinical studies and could serve as a basis for the development of methods for a better characterization of myocardial edema in clinical practice.

Sources of Funding

This work was supported by grants from the "Instituto de Salud Carlos III" (ISCIII) PI13/00398 and RD12/42/21. M.A.-V. received a fellowship from ISCIII, FI12/00411.

Disclosures

None.

References

1. Abdel-Aty H, Cocker M, Friedrich MG. Myocardial edema is a feature of Tako-Tsubo cardiomyopathy and is related to the severity of systolic dysfunction: insights from T2-weighted cardiovascular magnetic resonance. *Int J Cardiol*. 2009;132:291–293.
2. Abdel-Aty H, Cocker M, Meek C, Tyberg JV, Friedrich MG. Edema as a very early marker for acute myocardial ischemia: a cardiovascular magnetic resonance study. *J Am Coll Cardiol*. 2009;53:1194–1201.
3. Berry C, Kellman P, Mancini C, Chen MY, Bandettini WP, Lowrey T, Hsu L-Y, Aletras AH, Arai AE. Magnetic resonance imaging delineates the ischemic area at risk and myocardial salvage in patients with acute myocardial infarction. *Circ Cardiovasc Imaging*. 2010;3:527–535.
4. Puntmann VO, Taylor PC, Barr A, Schnackenburg B, Jahnke C, Paetsch I. Towards understanding the phenotypes of myocardial involvement in the presence of self-limiting and sustained systemic inflammation: a magnetic resonance imaging study. *Rheumatology (Oxford)*. 2010;49:528–535.
5. Sasaguri S, Sunamori M, Saito K, Suzuki A. Early change of myocardial water during acute cardiac allograft rejection. *Jpn Circ J*. 1986;50:1113–1119.
6. Davis KL, Mehlhorn U, Laine GA, Allen SJ. Myocardial edema, left ventricular function, and pulmonary hypertension. *J Appl Physiol*. 1995;78:132–137.
7. Mehlhorn U, Davis KL, Laine GA, Geissler HJ, Allen SJ. Myocardial fluid balance in acute hypertension. *Microcirculation*. 1996;3:371–378.
8. Aliev MK, Khatkevich AN, Tsyplenkova VG, Meertsuk FE, Kapelko VI. Tracer kinetics analysis of the extracellular spaces in saline perfused hearts. *Exp Clin Cardiol*. 2001;6:188–194.
9. Askenasy N, Tassini M, Vivi A, Navon G. Intracellular volume measurement and detection of edema: multinuclear NMR studies of intact rat hearts during normothermic ischemia. *Magn Reson Med*. 1995;33:515–520.
10. Askenasy N, Navon G. Measurements of intracellular volumes by 59Co and 2H/1H NMR and their physiological applications. *NMR Biomed*. 2005;18:104–110.
11. Eitel I, von Knobelsdorff-Brenkenhoff F, Bernhardt P, Carbone I, Muellerleile K, Aldrovandi A, Francone M, Desch S, Gutberlet M, Strohm O, Schuler G, Schulz-Menger J, Thiele H, Friedrich MG. Clinical characteristics and cardiovascular magnetic resonance findings in stress (takotsubo) cardiomyopathy. *JAMA*. 2011;306:277–286.
12. Joshi SB, Chao T, Herzka DA, Zeman PR, Cooper HA, Lindsay J, Fuisz AR. Cardiovascular magnetic resonance T2 signal abnormalities in left ventricular ballooning syndrome. *Int J Cardiovasc Imaging*. 2010;26:227–232.
13. Garcia-Dorado D, Théroux P, Munoz R, Alonso J, Elizaga J, Fernandez-Avilés F, Botas J, Solares J, Soriano J, Duran JM. Favorable effects of hyperosmotic reperfusion on myocardial edema and infarct size. *Am J Physiol*. 1992;262:H17–H22.
14. Bragadeesh T, Jayaweera AR, Pascotto M, Micari A, Le DE, Kramer CM, Epstein FH, Kaul S. Post-ischaemic myocardial dysfunction (stunning) results from myofibrillar oedema. *Heart*. 2008;94:166–171.
15. Butler TL, Egan JR, Graf FG, Au CG, McMahon AC, North KN, Winlaw DS. Dysfunction induced by ischemia versus edema: does edema matter? *J Thorac Cardiovasc Surg*. 2009;138:141–147.
16. Kloner RA, Ganote CE, Jennings RB. The 'no-reflow' phenomenon after temporary coronary occlusion in the dog. *J Clin Invest*. 1974;54:1496–1508.
17. Bekkers SCAM, Yazdani SK, Virmani R, Waltenberger J. Microvascular obstruction: underlying pathophysiology and clinical diagnosis. *J Am Coll Cardiol*. 2010;55:1649–1660.
18. Reffelmann T, Kloner RA. The no-reflow phenomenon: a basic mechanism of myocardial ischemia and reperfusion. *Basic Res Cardiol*. 2006;101:359–372.
19. Tranum-Jensen J, Janse MJ, Fiolet WT, Krieger WJ, D'Alnoncourt CN, Durrer D. Tissue osmolality, cell swelling, and reperfusion in acute regional myocardial ischemia in the isolated porcine heart. *Circ Res*. 1981;49:364–381.
20. Davis KL, Laine GA, Geissler HJ, Mehlhorn U, Brennan M, Allen SJ. Effects of myocardial edema on the development of myocardial interstitial fibrosis. *Microcirculation*. 2000;7:269–280.
21. Sugihara N, Genda A, Shimizu M, Suematu T, Kita Y, Horita Y, Takeda R. Quantitation of myocardial fibrosis and its relation to function in essential hypertension and hypertrophic cardiomyopathy. *Clin Cardiol*. 1988;11:771–778.
22. Ohsato K, Shimizu M, Sugihara N, Konishi K, Takeda R. Histopathological factors related to diastolic function in myocardial hypertrophy. *Jpn Circ J*. 1992;56:325–333.
23. Kellman P, Wilson JR, Xue H, Ugander M, Arai AE. Extracellular volume fraction mapping in the myocardium, part 1: evaluation of an automated method. *J Cardiovasc Magn Reson*. 2012;14:63.
24. Garcia-Dorado D, Oliveras J. Myocardial oedema: a preventable cause of reperfusion injury? *Cardiovasc Res*. 1993;27:1555–1563.
25. Fernández-Jiménez R, Sánchez-González J, Agüero J, García-Prieto J, López-Martín GJ, García-Ruiz JM, Molina-Iracheta A, Rosselló X, Fernández-Friera L, Pizarro G, García-Álvarez A, Dall'Armellina E, Macaya C, Choudhury RP, Fuster V, Ibáñez B. Myocardial edema after ischemia/reperfusion is not stable and follows a bimodal pattern: imaging and histological tissue characterization. *J Am Coll Cardiol*. 2015;65:315–323.
26. Inserte J, Garcia-Dorado D, Ruiz-Meana M, Solares J, Soler J. The role of Na+-H+ exchange occurring during hypoxia in the genesis of reoxygenation-induced myocardial oedema. *J Mol Cell Cardiol*. 1997;29:1167–1175.
27. Inserte J, Hernando V, Vilardosa Ú, Abad E, Poncelas-Nozal M, Garcia-Dorado D. Activation of cGMP/protein kinase G pathway in postconditioned myocardium depends on reduced oxidative stress and preserved endothelial nitric oxide synthase coupling. *J Am Heart Assoc*. 2013;2:e005975 doi: 10.1161/JAHA.112.005975.
28. Dou Y, Arlock P, Arner A. Blebbistatin specifically inhibits actin-myosin interaction in mouse cardiac muscle. *Am J Physiol Cell Physiol*. 2007;293:C1148–C1153.
29. Weinmann H, Brasch R, Press W, Wesbey G. Characteristics of gadolinium-DTPA complex: a potential NMR contrast agent. *Am J Roentgenol*. 1984;142:619–624.
30. Rodríguez-Sinovas A, García-Dorado D, Ruiz-Meana M, Soler-Soler J. Protective effect of gap junction uncouplers given during hypoxia against reoxygenation injury in isolated rat hearts. *Am J Physiol Heart Circ Physiol*. 2006;290:H648–H656.
31. Aliev MK, Dos Santos P, Hoerter JA, Soboll S, Tikhonov AN, Saks VA. Water content and its intracellular distribution in intact and saline perfused rat hearts revisited. *Cardiovasc Res*. 2002;53:48–58.
32. García-Dorado D, Oliveras J, Gili J, Sanz E, Pérez-Villa F, Barrabés J, Carreras MJ, Solares J, Soler-Soler J, Garcia-dorado D, Oliveras J, Gili J, Sanz E, Perez-villa F, Barrabks J, Carreras MJ, Solares J. Analysis of myocardial oedema by magnetic resonance imaging early after coronary artery occlusion with or without reperfusion. *Cardiovasc Res*. 1993;27:1462–1469.
33. Li T, Sperelakis N, Teneick RE, Solaro RJ. Effects of diacetyl monoxime on cardiac excitation-contraction coupling. *J Pharmacol Exp Ther*. 1985;232:688–695.
34. Garcia-Dorado D, Théroux P, Duran JM, Solares J, Alonso J, Sanz E, Munoz R, Elizaga J, Botas J, Fernandez-Avilés F. Selective inhibition of the contractile apparatus. A new approach to modification of infarct size, infarct composition, and infarct geometry during coronary artery occlusion and reperfusion. *Circulation*. 1992;85:1160–1174.
35. Garcia-Dorado D, Andres-Villarreal M, Ruiz-Meana M, Inserte J, Barba I. Myocardial edema: a translational view. *J Mol Cell Cardiol*. 2012;52:931–939.
36. Fernández-jiménez R, Sánchez-gonzález J, Aguero J, Trigo M, Galán-arriola C, Fuster V, Ibáñez B. Fast T2 gradient-spin-echo (T2-GraSE) mapping for myocardial edema quantification: first in vivo validation in a porcine model of ischemia/reperfusion. *J Cardiovasc Magn Reson*. 2015;17:92. DOI 10.1186/s12968-015-0199-9